

Analysis of the pore-size distribution and fiber saturation point of native and thermally modified wood using differential scanning calorimetry

Mario Zauer · Jens Kretzschmar · Livia Großmann ·
Alexander Pfriem · André Wagenführ

Received: 4 March 2013 / Published online: 25 October 2013
© Springer-Verlag Berlin Heidelberg 2013

Abstract The aim of this paper was to investigate pore-size distributions in the nano-diameter range of wood and their alteration due to thermal modification of wood using thermoporosimetry, and to find out what consequences can be derived regarding the biological durability. Thermoporosimetry is a technique that is based on the measurement using differential scanning calorimetry (DSC). The method is based on the fact that frozen water contained within small pores is at elevated pressure and therefore has a depressed melting temperature as a function of the appropriate pore diameter. In addition, the fiber saturation points (FSP) were determined by DSC. The former were performed in an isothermal-step method and the latter using the continuous heating-up method. Native and thermally modified twin samples of Norway spruce (*Picea abies* (L.) Karst.), Sycamore maple (*Acer pseudoplatanus* L.) and European ash (*Fraxinus excelsior* L.) were analyzed. The results clearly show that the pore shares of wood for the measurable diameter range between 4 and 400 nm decrease considerably in all studied wood species due to thermal modification of the wood. Furthermore, thermal modification of wood leads to a decreased FSP for all studied wood species. For evaluation as well as reproducibility of the results of pore-size distribution and FSP, the consideration of sensible heat and specific heat of fusion plays an important role. If this is not done, it can lead to misinterpretations.

M. Zauer (✉) · L. Großmann · A. Wagenführ
Institute of Wood and Paper Technology, Technische Universität Dresden, 01062 Dresden,
Germany
e-mail: mario.zauer@tu-dresden.de

J. Kretzschmar
Papiertechnische Stiftung (PTS), Heidenau, Germany

A. Pfriem
Eberswalde University for Sustainable Development, Eberswalde, Germany

Introduction

Thermal modification of wood is a heat treatment of wood and is aimed mainly at improving the biological durability and increasing the dimensional stability (Hill 2006). This procedure currently is the most advanced modification process for alternative wood preservation. The various methods for thermal modification of wood differ substantially in the engineering process and atmospheric conditions in the treatment chamber. For example, steam, nitrogen, vegetable oil (partly in combination with different pressures: over-pressure, normal pressure, vacuum) are used to minimize the oxygen content for realization of a mild pyrolysis of the wood components. In dependence of the atmospheric conditions, at the same treatment time and temperature, the resulting alterations in the properties of wood differ significantly. During the thermal treatment, the cell-wall components cellulose, hemicelluloses and lignin are degraded or transformed. As a consequence of the degradation processes, the wood loses some of its mass (Pétriassans et al. 2012). The hemicelluloses as thermally unstable components are mostly degraded. Furthermore, due to oxidation and condensation processes self-crosslinking of the cell-wall components can occur (Wagenführ and Scholz 2007). Thus, the porosity and pore-size distribution of the wooden cell-wall as well as of the various voids in the wood structure (e.g. pointed ends of the lumen, pit apertures, pit membrane voids) are modified. Furthermore, due to the primary degradation of the very hygroscopic hemicelluloses and also the irreversible hornification (Kürschner and Melcerová 1965; Roffael and Kraft 2012) of the cell wall, the fiber saturation point (FSP) is decreased due to thermal modification. In general, the increased biological durability of thermally modified wood can be explained by different active principles. On the one hand, toxic substances, such as furfural and formaldehyde (Peters et al. 2008; Tjeerdsma et al. 1998) are developed during the thermal modification process. On the other hand, due to the degradation and especially the transformation of the cell-wall substances, the enzymes of wood-decaying fungi cannot take effect. Furthermore, due to thermal modification, cell-wall porosity is reduced, which can limit diffusion of cellulolytic enzymes into the cell walls (Lekounougou 2009). Hence, it is possible that the proportion of capillary condensed water in the nano-pores decreases due to thermal modification. That means that the ratio of water for enzymatic activity is probably limited compared to native wood even below FSP. Therefore, the knowledge of the alteration of the pore-size distribution of the pores in which water capillary condensation can occur due to thermal modification is of high importance to discuss the improved biological durability of thermally modified wood. Its determination in this work was carried out using thermoporosimetry.

The basis of thermoporosimetry to measure pore-size distribution using DSC is the melting point depression of a pore-filling substance or adsorbate in very small pores (Maloney 2000; Książczak et al. 2003), which occurs by osmotic and capillary effects (Topgaard and Söderman 2002). Because of the increased internal pressure, a depressed melting temperature occurs in the interior of small pores (Stephan et al. 2010). On the assumption that all pores are cylindrical, the relationship between the pore diameter and the melting-point depression will be described by the Gibbs-

Thomson Eq. (1) (Landry 2005). From this equation it is evident that with decreasing pore diameter, the melting point depression increases.

$$D = \frac{4T_m\gamma \cos \theta}{(T_m - T_m(D))\rho H_f} \quad (1)$$

where T_m is the melting temperature, γ is the surface tension, θ the contact angle, ρ the density and H_f the specific heat of fusion of water. Since the melting point depends on the pore diameter, a determination of pore-size distribution in the nano-diameter range using DSC is possible. To determine the pore-size distribution using DSC, water as pore-filling substance is well suited because of the well-known anomaly of water and its melting point of 0 °C. The water in the pore structure of wood or other ligno-cellulosic materials is generally divided into bound water in the hygroscopic region below FSP and free water in the over-hygroscopic region above FSP. In contrast, for DSC measurements water must be divided into three types: non-freezing bound water (nfbw), freezing bound water (fbw) and free water (fw) (Książczak et al. 2003). The former is bound by chemisorption and adsorption as a layer surrounding the microfibrils with approximately 1 nm thickness (Topgaard and Söderman 2002) and cannot freeze because of its strong bonds. Thus, this water has consequently no melting peak in the DSC measurement curve (Park et al. 2006). On the one hand, fbw is stored by capillary condensation in the intermicellar and interfibrillar cavities of the cell wall and on the other hand in small pore spaces outside the cell wall, such as the pointed ends of the lumen, pits apertures and pit-membrane voids. The embedded free water in the lumen of the wood cells undergoes no melting point depression (Książczak et al. 2003).

To apply the thermoporosimetry on cellulosic and inorganic porous material, some investigations have already been carried out. Maloney and Paulapuro (1999) studied the pore-size distribution depending on the degree of cooking of pulped spruce. They found that the pore sizes are significantly enlarged due to delignification. Park et al. (2006) examined the alteration of the pore-size distributions of cellulose as a function of the degree of drying of the fibers, and Fahlén and Salmén (2005) examined the alteration due to an enzymatic treatment on various fibrous materials. The former authors determined varying pore-size distributions in dependence of the moisture content (MC) in the over-hygroscopic region, whereby with decreasing MC the pore diameters are decreased. All three groups of authors performed their measurements based on Maloney (2000) using an isothermal temperature step program.

Simpson and Barton (1991) focused their work on the determination of the fiber saturation point (FSP) of several Australian wood species (e.g. *Eucalyptus marginata*) in consideration of the wood planes, while Repellin and Guyonnet (2005) investigated the alteration of FSP due to thermal modification on common beech and maritime pine and compared the results to those obtained by volumetric shrinkage. For these studies the experiments were carried out using a continuous heating program. The former authors found no significant statistical differences between the three wood planes of the samples and the latter authors determined a decrease of FSP due to thermal modification as a function of treatment temperature and time. Furthermore, the

correlation of the DSC method with volumetric shrinkage method shows a linear regression.

Weise et al. (1996) used DSC for the quantification of the three types of water (nfbw, fbw and fw) in different kraft pulps which were moistened and subsequently dried again. The aim of this study was to investigate the hornification of the cellulose fibers due to dehydration. The separation of fbw and fw was taken by a vertical separation of both the overlapping melting peaks at the local minimum, which visually separates both melting peaks. Dieste et al. (2009) followed a different approach in their investigations on DMDHEU (1,3-dimethylol-4,5-dihydroxy ethylene urea) treated beech particles. Based on Park et al. (2006), they assumed that the melting point depression in wood also depends on the MC of the sample. Therefore, the samples were prepared with different moisture contents and measured with a continuous measurement program. The evaluation was performed using the determination of the extrapolated onset temperature at the melting peak of the fbw. Thus, the respective average melting temperature or the average pore diameter was determined respectively. The representation of the results was shown by defined pore classes. However, it should be noted that the average pore diameter above FSP was determined by chance and not as a function of moisture content. The results of Park et al. (2006) may be explained by the collapse of the lumen of the cellulosic fibers due to dehydration and associated suction. As a result of lignin in the cell wall of the wood particle, this phenomenon is very limited and occurs only due to very excessive drying. Zelinka et al. (2012) examined the freezing of water in wood and its cell-wall components under a variety of preparation methods. They reported that the detection of freezable bound water or “Type II water” in wood may depend more on the sample preparation than the chemical nature of the cell-wall components. Only for ball-milled cellulose they could determine a DSC peak for Type II, not for milled and solid wood (*Pinus taeda*). The authors derive from their investigations that Type II water is not a result of fbw, but can be explained by homogenous nucleation in water. Furthermore, in the mentioned study, FSP were determined from the melting enthalpy using heating up measurements.

In all mentioned studies the heating rates were very different. Weise et al. (1996), Maloney (2000), Repellin and Guyonnet (2005) and Park et al. (2006) have aimed at a pretty low heating rate in the range between 0.5 and 3 K min⁻¹. Simpson and Barton (1991) or Zelinka et al. (2012) used a setting of 5 K min⁻¹. In contrast, Dieste et al. (2009) used a quite high heating rate of 10 K min⁻¹. Maloney and Paulapuro (1999) or Fahlén and Salmén (2005) described no values for the heating rate.

Materials and methods

General aspects

The investigations were carried out on native and thermally modified heartwood of Norway spruce (*Picea abies* (L.) Karst.), Sycamore maple (*Acer pseudoplatanus* L.) and European ash (*Fraxinus excelsior* L.). The thermal modification was performed in a single-stage dry process under nitrogen atmosphere at 200 °C for 4 h at

laboratory scale. Twin samples of unmodified and modified wood collected from the same annual rings were analyzed. In addition, the series differ from each other in terms of sample shape. On the one hand, samples were prepared as particles (size fraction between 0.8 and 1 mm) and on the other hand as solid wood sections (cross-cut sections) with a diameter of 4 mm in the radial-tangential section and 1 mm in longitudinal direction. The particles were milled using a hammer mill and the cross-cut sections were cut using a slicing machine and a steel punch. The preparation of the modified wood samples was performed after thermal treatment of the twin plank. Each test series comprised three specimens.

The DSC-measurements were carried out using the DSC-1-STARe-system with Intracooler (Co. METTLER TOLEDO), the evaluation of the measurement curves using STARe software V 9.20. Temperature calibration of the DSC-analyzer was performed by two-point calibration with mercury (melting point $-38.4\text{ }^{\circ}\text{C}$) and deionized water (melting point $0\text{ }^{\circ}\text{C}$). Technically pre-dried air (4 % relative humidity at $20\text{ }^{\circ}\text{C}$) was used as scavenging gas; the flow rate was 40 ml min^{-1} . Standardized aluminum pans (Co. METTLER TOLEDO) with a center pin and a capacity of $40\text{ }\mu\text{l}$ were used. In the lid of the empty and initially hermetically sealed reference pan, two small holes were poked. Thus, the reference substance was air. Weighing of the samples, pans and lids was performed using a balance (Co. METTLER TOLEDO) with a precision of 0.01 mg. In each case, the average of three weighings was calculated. Each mass of the pans and lids for the same test were determined separately from the samples. In water dissolved substances, such as soluble sugars in the wood, lead to an additional melting point depression. Therefore, samples were washed in deionized water and stored in the water for 24 h. Before weighing, water saturated samples were stored on a wet filter paper for two minutes. Subsequently, samples were placed in the pans before being hermetically sealed. After the DSC-measurements, a small hole was poked through the lid of the pan and the sample was dried at $103\text{ }^{\circ}\text{C}$. The mass of the sample before drying and in the oven-dry state were used to calculate the MC of the samples.

In the previous studies mentioned above, different initial temperatures in the range between -10 and $-40\text{ }^{\circ}\text{C}$ were used. To select an appropriate initial temperature, several investigations using the heating up method with a heating rate of 3 K min^{-1} on water saturated cross-cut sections of native spruce were carried out. The initial temperatures were -20 and $-70\text{ }^{\circ}\text{C}$ and the end temperature in each case was $10\text{ }^{\circ}\text{C}$. The tests were conducted twice per initial temperature. Figure 1 shows the determined melting curves at the different initial temperatures. The results clearly show that the first deviation of the melting curve from the baseline occurred in each case at $-10\text{ }^{\circ}\text{C}$, regardless of the initial temperature. The determined integrated areas or the enthalpy also have the same values. For the present study it was assumed that at temperatures below $-10\text{ }^{\circ}\text{C}$ no pore water melts, thus no latent heat is consumed for the endothermic process.

Pore-size distribution

The determinations of the pore-size distribution were carried out using an isothermal step method according to Park et al. (2006) as well as Maloney and

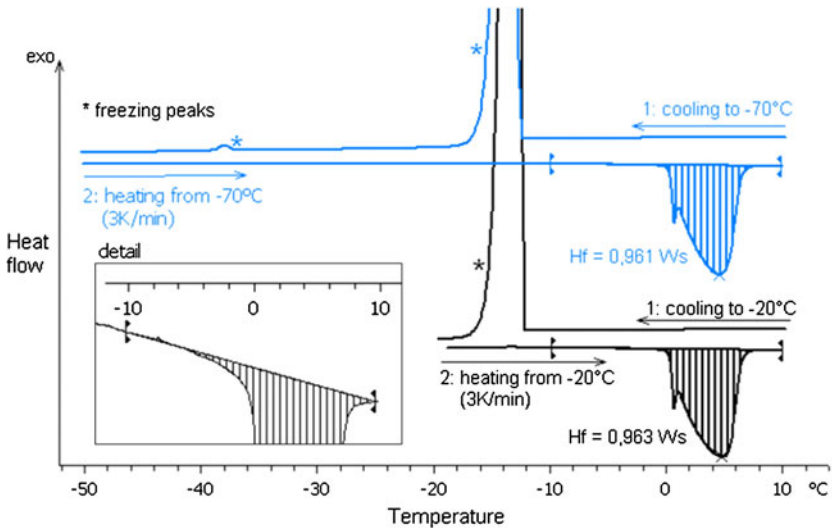


Fig. 1 DSC-melting curves with continuous heating up at different start temperatures: $-20\text{ }^{\circ}\text{C}$ and $-70\text{ }^{\circ}\text{C}$

Paulapuro (1999). However, in contrast to these authors an initial temperature of $-20\text{ }^{\circ}\text{C}$ was used in the present study. This is due to the results of the preliminary investigation mentioned above using different initial temperatures (-20 and $-70\text{ }^{\circ}\text{C}$) where the first deviation of the melting curve from the baseline was always at $-10\text{ }^{\circ}\text{C}$. Likewise, the determination of the pore-size distribution started from $-10\text{ }^{\circ}\text{C}$. To ensure that the freezing water is completely frozen, the start temperature was initially held constant for 5 min. In each step, the temperature was increased using a heating rate of 2 K min^{-1} and the respective temperature step was held for 3 min. To calculate the effective pore diameter according to Eq. 1, the following parameters were used: $T_m = 273.15\text{ K}$; $\gamma = 12.1\text{ mJ m}^{-2}$; $\theta = 180^{\circ}$; $\rho = 10^6\text{ g m}^{-3}$; $H_f = 333.6\text{ J g}^{-1}$ (Park et al. 2006; Stephan et al. 2010; Simpson and Barton 1991). Thus, the individual pore diameters were calculated suitably according to Eq. 2. Table 1 shows the 15 temperature steps used and the corresponding measurable pore diameter between 4 and approximately 400 nm.

$$D = 39.6\text{ nm} \times \frac{K}{T_m - T_m(D)} \quad (2)$$

To prepare an empirical distribution function of the individual pore sizes, it is necessary to determine the total individual heats of fusion $H_{m,i,\text{total}}$ of the respective endothermic melting peak of each temperature step. This was achieved by integration of the corresponding peak area. Based on the preliminary investigations in this study, it was assumed that the individual melting peaks before $-10\text{ }^{\circ}\text{C}$ are attributed to sensible heat as a result of inertia of the sample due to delayed increase in temperature of the sample. Maloney (2000) reported that for the precise determination of the actually consumed melting heat (latent heat), the occurring sensible heat must be subtracted from the determined total heat of fusion ($H_{m,i,\text{total}}$).

Table 1 Comparison of the used melting temperatures and corresponding pore diameters due to the Gibbs-Thomson effect (Eqs. 1 and 2)

T_m (°C)	D (nm)
-10	4.0
-9	4.4
-8	5.0
-7	5.7
-6	6.6
-5	7.9
-4	9.9
-3	13.2
-2	19.8
-1.5	26.4
-1.1	36.0
-0.8	49.5
-0.5	79.3
-0.2	198.2
-0.1	396.3

Here, the function of the sensible heat depending on the temperature below 0 °C can be assumed to be directly proportional and increases with increasing temperature. On this account, $H_{m,i,\text{total}}$ is the sum of sensible heat $H_{SH,i}$ of the sample and the actual (latent) heat of fusion $H_{m,i}$, which is actually consumed for the melting process of frozen water in the corresponding pore diameter (Maloney 2000; Park et al. 2006) (Eq. 3).

$$H_{m,i,\text{total}} = H_{m,i} + H_{SH,i} \quad (3)$$

The general calculation of sensible heat (H_{SH}) results from the temperature-dependent specific heat capacity c_p (T), the temperature difference of the corresponding temperature step ΔT and the sample mass m_s according to Eq. 4.

$$H_{SH} = c_p * \Delta T * m_s \quad (4)$$

In the temperature range below 0 °C, H_{SH} is directly proportional to the temperature (Aristov et al. 2010), where H_{SH} values decrease with decreasing temperature. In this study, also a linear function was assumed. Hence, H_{SH} were determined at each 1 K step between -20 and -11 °C. The proportions of the frozen water v_i of the corresponding pore diameter were calculated according to Eq. 5:

$$v_i = \frac{H_{m,i}}{H_f * \rho * m_0} \quad (5)$$

where m_0 is the mass of the oven-dry sample. To calculate v_i the same parameters (H_f , ρ) as described above were used.

Fiber saturation point

The determinations of FSP were carried out using the continuous heating-up method and subsequently the investigation of pore-size distribution on the same sample.

Again, the start temperature of $-20\text{ }^{\circ}\text{C}$ was held for 5 min and the temperature was then increased to $10\text{ }^{\circ}\text{C}$ using a heating rate of 2 K min^{-1} . According to Simpson and Barton (1991) the calculation of FSP was performed using two different methods. FSP is defined as the moisture content, where the cell wall is fully saturated without capillary condensed water in the cell-wall pores (Siau 1995; Almeida and Hernández 2006; Hill 2008). Following this, in method 1 the FSP was determined by calculating the amount of non-freezing water (NFW) according to Eqs. 6 and 7:

$$\text{FSP} = \text{NFW} = \left(\frac{m_s - m_{\text{FW}}}{m_0} - 1 \right) \times 100 \quad (6)$$

with:

$$m_{\text{FW}} = \left(\frac{\Delta H_m * m_s}{H_f} \right) \quad (7)$$

where m_s is the mass of the sample (mg), m_{FW} is the mass of the freezing water (mg) and m_0 is the mass of the oven-dry sample (mg), ΔH_m is the determined total heat of fusion (J g^{-1}), H_f is the specific heat of fusion of pure water (J g^{-1}). On the one hand, fw was assumed to behave like pure water, thus the accepted value of 333.6 J g^{-1} (Park et al. 2006; Simpson and Barton 1991; Repellin and Guyonnet 2005; Dieste et al. 2009) was used for H_f . On the other hand, in accordance with Simpson and Barton (1991), pure water-only scans were carried out and a value of 324.4 J g^{-1} was determined using regression analysis depending on the mass of water. This H_f was also used for the calculation of FSP.

In method 2, the measured specific heat of fusion of the corresponding series was plotted against the water content of the sample and linearly regressed using the method of least squares. Thus, in each case the regression equation with the corresponding coefficient of determination was determined and the proportion of non-freezing bound water (nfbw) in a heat of fusion of 0 J g^{-1} was calculated. This means that the FSP was determined by extrapolating the regression line of any sample when the H_f value is zero (Simpson and Barton 1991; Zelinka et al. 2012).

Results and discussion

Pore-size distribution

The average pore-size distribution (cumulative pore volume) of native and thermally modified spruce, maple and ash particles and sections, taking into account the H_{SH} , are shown in Figs. 2, 3 and 4. The specified pore volume refers to the oven-dry mass of the sample. The results clearly show that the pore-size distributions differ in dependence of shape (particles, sections) and state (native, modified) of the samples. The respective pore shares of the particles were always higher compared to the values of the solid wood sections. This is likely to be explained by the better accessibility and free swelling ability of the individual

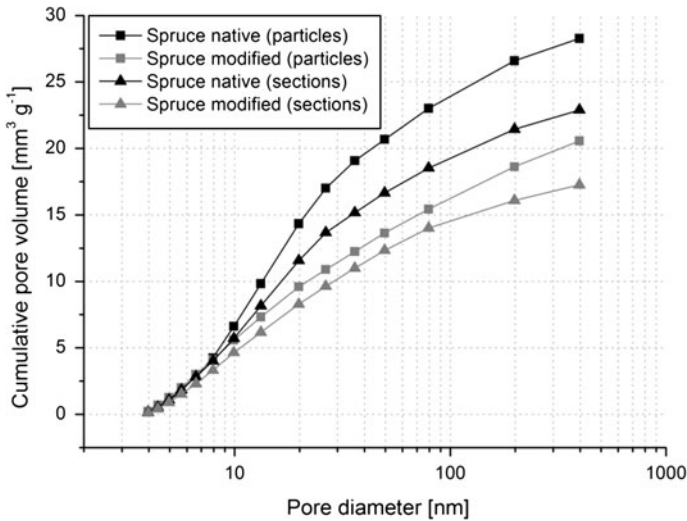


Fig. 2 Average cumulative pore-volume curves of native and thermally modified spruce particles and sections

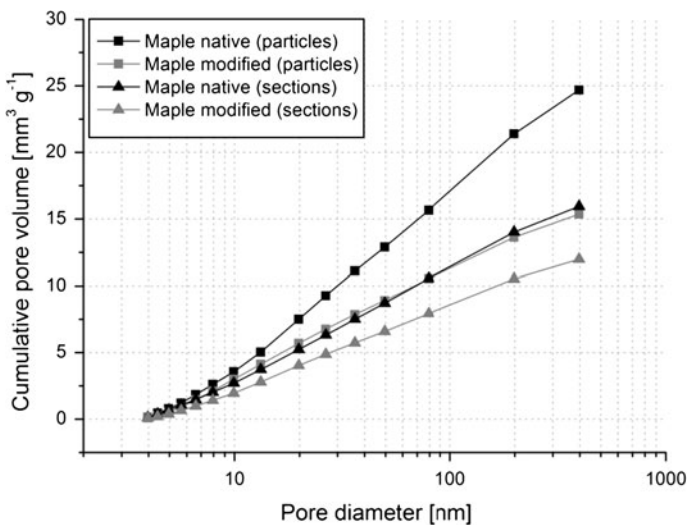


Fig. 3 Average cumulative pore-volume curves of native and thermally modified maple particles and sections

wooden cell walls of the individual particles (Maloney and Paulapuro 1999) compared to the individual cells in the composite of the solid wood sections. Furthermore, the contact points of each chip may have produced additional voids. A significant result of thermoporosimetry is that the pore shares for the pore diameter range between approximately 4 and 400 nm decrease considerably in all studied wood species due to thermal modification. The cause may be the shrinkage of the

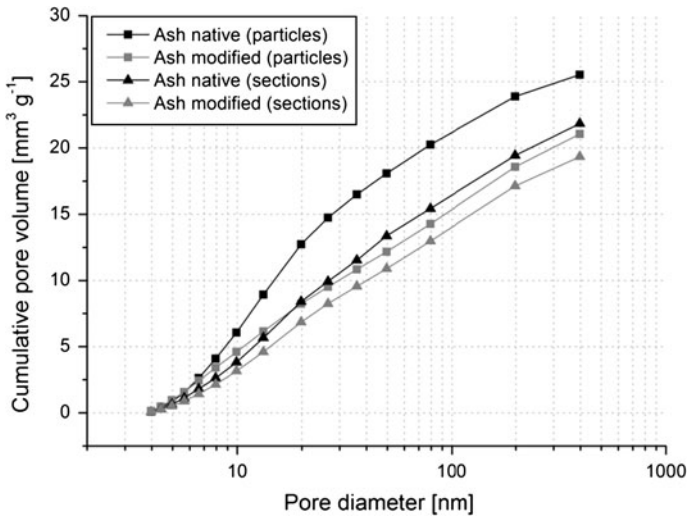


Fig. 4 Average cumulative pore-volume curves of native and thermally modified ash particles and sections

cell wall (Zauer et al. 2013), flowing of lignin in the cell-wall pores as well as reduced swelling behavior of thermally modified wooden cell walls and resulting reduced interfibrillar and intermicellar spaces. This effect was likely to be amplified due to hornification during thermal modification, which was detected by Kürschner and Melcerová (1965). Furthermore, Kollmann and Fengel (1965) suggested a closure of the skeletal substance of wood due to softening and subsequent solidification of lignin during thermal treatment. A substantial portion of the pore-size distributions can be assigned to the pointed ends of the previously mentioned cell elements. This decreases obviously due to the thermal modification, which is attributable to the shrinkage of the cell walls and thus the cell lumen or pit chambers, respectively, at their pointed ends. In addition, pit-membranes were degraded due to thermal modification so that the presence of small “nano” voids was reduced significantly. Figure 5 shows an intact bordered pit of spruce and a degraded pit due to thermal modification. It can be clearly seen that the pit membrane gets larger pores due to degradation processes during thermal treatment compared to the native pit membrane (closer meshed). A significant ratio of the voids of the thermally treated pit membrane has a diameter above 400 nm and cannot be determined using thermoporosimetry. From these results it can be derived that the proportion of capillary condensed water in the cell wall and “nano” pores outside of the cell wall in thermally modified wood is significantly lower compared to native wood. Thereby, the proportion of water in the hygroscopic region for fungi-specific enzymatic activity is clearly decreased. Furthermore, the reduced porosity can limit diffusion of enzymes into the cell wall (Lekounougou 2009). In addition to the phenomena mentioned above, these are obviously important facts of the improved biological durability of thermally modified wood compared to native wood.

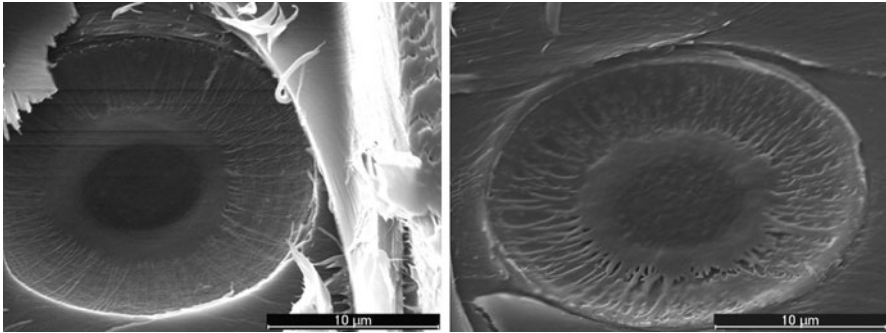


Fig. 5 Alteration of the pit membrane or torus of spruce due to thermal modification: intact bordered pit (*left*) and changes as well as degradation of margo and torus (*right*)

In this study, a depression temperature of $-0.1\text{ }^{\circ}\text{C}$ as the closest temperature below the normal freezing point of water ($0\text{ }^{\circ}\text{C}$) was chosen. All average cumulative pore-volume curves (Figs. 2, 3, 4) show no plateau in the region of larger pore sizes. This indicates that there is a significant amount of pores larger than 396 nm present in the native and thermally modified wood samples. Park et al. (2006) also found this phenomenon on softwood fully bleached kraft pulp. The larger pores above 396 nm in wood are probably in the pointed ends of lumens and pit apertures, openings in the pit margo, especially of softwood with a width up to $1\text{ }\mu\text{m}$ in the circumferential direction and up to $2\text{ }\mu\text{m}$ in the radial direction (Siau 1995). A comparison of the native wood samples shows that maple has slightly lower pore shares in the investigated pore range compared to spruce and ash.

As mentioned above, Figs. 2, 3 and 4 represent the cumulative pore-volume curves taking into account H_{SH} . However, in some investigations on pore-size distribution, H_{SH} has not been considered (Maloney and Paulapuro 1999; Fahlén and Salmén 2005; Weise et al. 1996). The maximum cumulative pore volume of this study ranged between 12 (modified maple sections) and $22\text{ mm}^3\text{ g}^{-1}$ (native spruce particles). For spruce particles, Fahlén and Salmén (2005) determined a maximum cumulative pore volume of $500\text{ mm}^3\text{ g}^{-1}$, and Maloney and Paulapuro (1999) determined a maximum cumulative pore volume of $250\text{ mm}^3\text{ g}^{-1}$. This means that the values are higher by a decimal power compared to the values of this study. It should be noted, that the depression temperature ranged between -33 (-30) and $-0.1\text{ }^{\circ}\text{C}$, contrary to the present work (-10 and $-0.1\text{ }^{\circ}\text{C}$). But the individual pore volumes up to approximately $-10\text{ }^{\circ}\text{C}$, corresponding approximately to a pore diameter of up to 4 nm , were very low compared to the individual pore volumes above $-10\text{ }^{\circ}\text{C}$. The main reason for the higher individual pore volume compared to the present values is obviously that the H_{SH} was not accounted for. If the pore volume of this study had been calculated without taking into account H_{SH} , the maximum pore volume would have ranged between 125 (modified ash sections) and $280\text{ mm}^3\text{ g}^{-1}$ (native maple particles). These values are similar to the results of Maloney and Paulapuro (1999). However, H_{SH} is an important influential parameter, which is necessarily taken into account when calculating the individual pore

volume. If H_{SH} is not considered, the pore shares of the sample are incorrectly determined too high.

Park et al. (2006) were the only ones that considered H_{SH} in the calculation of the pore-size corresponding pore volume. Because the investigations were carried out in bleached kraft pulp of pine, the values are not comparable to the values of the present study. Unpublished investigation of the authors on kraft pulp of a mixture of spruce and pine yielded a maximum pore volume under consideration of H_{SH} , of approximately $160 \text{ mm}^3 \text{ g}^{-1}$. The maximum pore volume of Park et al. (2006) ranged between 130 and $320 \text{ mm}^3 \text{ g}^{-1}$ depending on the MC of the pulp fibers, thus they are similar to unpublished results (Zauer 2011) on pulp. The results show that the pore volumes of wood are considerably lower compared to kraft pulp. This is mainly caused by the delignification during the pulping process and the dissolution of hemicelluloses, resulting in additional voids between the interfibrillar and intermicellar spaces.

Fiber saturation point

Figure 6 (left) shows a perfect example of the DSC-melting curve determined by a continuous heating up method, exemplary of native ash sections, and represents qualitatively all melting curves of the sample sections. The curve clearly shows two melting peaks, where the first peak occurs due to the melting point depression of fbw and the second peak reflects the proportion of fw. However, the first peak of the melting curve of the particles (Fig. 6 right) is not as pronounced as the first peak of the sections. In general, a better resolution of two peaks can be achieved at lower heating rates and a lower sample mass (Simpson and Barton 1991). From the analysis of controlled-pore glass standards (Landry 2005) a very slow scan rate even of 0.05 K min^{-1} is advised. However, it should be noted that at very slow scan rates the resulting measured signals show noise and are difficult to evaluate reproducibly. Additionally, the contact between the sample and the pan bottom is very important for exact measurements and precise measurement curves. Samples with a high degree of fineness, such as ball milled wood, are probably more suitable.

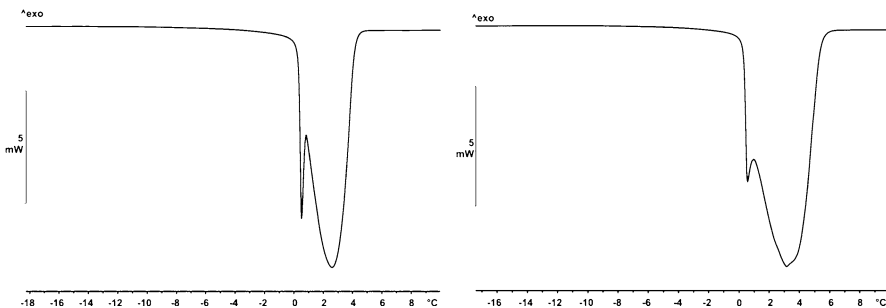


Fig. 6 DSC-melting curve with continuous heating up measured on native ash sections (*left*) and particles (*right*) for determining FSP

Table 2 Average fiber saturation [%] point of native and thermally modified spruce, maple and ash in dependence of sample shape and method of specific heat of fusion

Wood species	State	Sample shape	Method 1		Method 2	
			$H_f = 333.6 \text{ J g}^{-1}$	$H_f = 324.4 \text{ J g}^{-1}$	$H_f [\text{J g}^{-1}]$	
Spruce	Native	Particles	38.3	32.5	38.0	334.6
		Sections	36.3	32.4	35.9	333.2
	Modified	Particles	33.0	25.6	25.8	322.8
		Sections	32.1	25.8	25.8	321.3
Maple	Native	Particles	38.2	33.3	41.0	333.1
		Sections	37.4	33.9	37.1	332.6
	Modified	Particles	31.4	26.1	27.6	325.2
		Sections	30.0	27.0	27.1	323.9
Ash	Native	Particles	38.6	35.4	37.5	329.9
		Sections	37.1	35.5	37.6	331.6
	Modified	Particles	32.9	31.5	26.2	322.8
		Sections	31.5	29.6	25.3	321.2

Table 2 presents the average FSP of native and thermally modified spruce, maple and ash in dependence of the sample shape (particles, sections) and the calculation method (1, 2). Additionally for method 2, the respective calculated H_f are given. As expected, all results show a significant reduction in FSP due to thermal modification, which is mainly caused by the irreversible degradation of thermally sensitive hemicelluloses. It cannot be excluded that chemical changes of lignin and the formation of lignin-carbohydrate complexes cause a significant reduction in FSP (Repellin and Guyonnet 2005). In addition, the contact angle has a significant impact especially on capillary condensation (Kollmann and Fengel 1965), which increases during thermal modification and thus the wettability is reduced. Furthermore compared to cross-cut sections, the FSP of particles shows slightly higher values. Due to sieve-fractionation through the mesh (0.8 mm), it is possible that brittle proportions of lignin were separated from the particles and consequently the proportion of cellulose and hemicelluloses was increased. A high influence of the increased FSP of the particles probably creates better accessibility of the particles compared to the sections, whereby the free swelling capacity of the individual cell walls of the wood is improved (Maloney and Paulapuro 1999).

However, although Repellin and Guyonnet (2005) used the same H_f (333.6 J g^{-1}) in method 1, the determined FSP are significantly lower than the results of this study. For example, the measured FSP using DSC of the mentioned authors were 32.9 % for native European beech and 31.7 % for native Maritime pine. Likewise, the values for the thermally modified samples, exemplified for thermally modified beech with a treatment temperature of $200 \text{ }^\circ\text{C}$ and a treatment time of 3 h (FSP of 22.0 %), are significantly lower in comparison to the FSP of this work. The authors also used a heating rate of 2 K min^{-1} , but in contrast to the measurements of the present investigations a different initial temperature ($-40 \text{ }^\circ\text{C}$)

and end temperature (40 °C). However, preliminary investigations of this study clearly show that, independent of the start temperature (−70 or −20 °C), the first deviation from the baseline always occurred at −10 °C and the determined integration areas, thus the enthalpy, also showed no differences. Simpson and Barton (1991) determined FSP of approximately 38 % for different eucalyptus species (Jarrah and Karri) and FSP of approximately 28 % for pine using DSC and the same H_f (333.6 J g^{−1}). Maloney and Paulapuro (1999) determined FSP of approximately 37 % for untreated spruce fibers and Weise et al. (1996) FSP of approximately 38 % for thermo mechanically pulped (TMP) fibers and thus also significantly higher values compared to Repellin and Guyonnet (2005).

The assumptions of the accepted value for H_f of 333.6 J g^{−1} has probably not fully taken into account all freezing water in the samples. Due to the melting point depression in the pores with a diameter of less than 400 nm, it is possible that the fbw has a lower H_f compared to pure water. In addition, dissolved substances, such as organic or inorganic extractives, can also reduce H_f significantly. As a consequence of the reduced H_f , the calculated mass of fw (Eq. 6) increases, thus the proportion of NFW respectively FSP (Eq. 2) is reduced. The FSP calculated using H_f of 324.4 J g^{−1} are significantly lower compared to the FSP calculated using H_f of 333.6 J g^{−1}. Furthermore, the results of each series show the same value independent of the sample shape (particles, sections).

For method 2 in Fig. 7, a general review regarding the function between the measured H_f from the MC of the sample, independent of the wood species, sample shape and state (native, thermally modified) is presented. In contrast to the approach of Simpson and Barton (1991), H_f and MC are based on the oven-dry mass (Zelinka et al. 2012). The results clearly show a significant linear relationship (with $r^2 = 0.998$) between H_f and MC of the samples. Thus for each series, a separate linear regression was performed and extrapolated MC at H_f of 0 J g^{−1} was defined as FSP. Although for each regression r^2 was at least 0.97, it should be noted that each series included only three samples. Thus, it could not provide statistically significant values. However, a comparative analysis should rather be made hereby compared to method 1 because the measured values using method 2 were based on really measured specific heats of fusion. Likewise, a significant difference between native and thermally modified wood can be seen. FSP of thermally modified wood samples determined using method 2 are clearly lower (at least 10 % MC) than FSP of native samples compared to the results calculated using method 1. The reason of this phenomenon is the lower H_f determined consequently for all thermally modified wood samples (Table 2). The H_f for all native wood samples are similar to the accepted value for H_f of 333.6 J g^{−1} and H_f for all thermally modified wood samples are similar to the determined value of pure water-only scans (324.4 J g^{−1}). This indicates a significant influence of the thermal modification on the hygroscopicity of the wood. Zelinka et al. (2012) determined FSP of 27 % for loblolly pine (*P. taeda*) using method 2. However, in contrast to the present study they used a higher heating rate of 5 K min^{−1} as well as lower initial temperature (−65 °C) and higher end temperature (25 °C).

In general, the determined FSP were partly significantly higher compared to generally accepted assumptions.

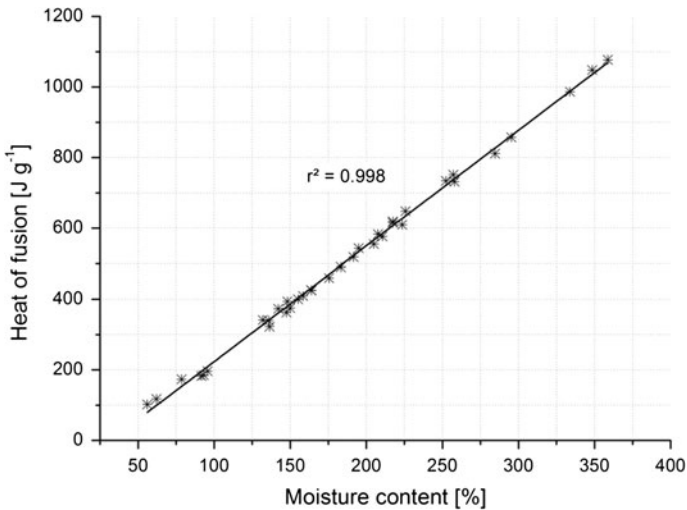


Fig. 7 Comparison of the measured specific heats of fusion of all series in dependence of the moisture content of the sample based on oven-dry mass of the samples

The average FSP of woods growing in the temperate zone often is assumed to be approximately 30 % (Siau 1995). However, this value can be assumed when wood is conditioned (adsorption) from a state below 100 % RH, thus in the hygroscopic region of the wooden cell wall. The swelling processes during adsorption are particularly hampered by the crystalline areas of the cellulose and lignin matrix. Furthermore, the intermolecular hydrogen bonds between the cellulose chains create a prestressing, which are more pronounced at lower MC of wood than higher MC of wood. Thus, the swelling as well as the water vapor absorption of wood is hindered. Accordingly, the intermicellar and interfibrillar spaces are smaller than those of desorption. In addition, the wettability of the dry state is considerably less in contrast to the wetter state of the cell wall (Chen and Wangaard 1968). As a consequence, less water can be bound. Thus, the well-known hysteresis between adsorption and desorption isotherm is formed, in which the respective MC of desorption is higher than the MC of adsorption (Aristov et al. 2010). The samples for the DSC measurements were initially water saturated. Thus, the cell wall of each sample was in the fully swollen state and the availability of bonding sites of sorption on molecular surfaces (Chen and Wangaard 1968) is higher compared to wood samples conditioned in the hygroscopic region. Therefore, FSP, for instance measured by desorption of never-dried wood, is higher than FSP measured by adsorption of oven-dried wood. Babiak and Kudela (1995) described different methods for determining FSP, where the individual FSP vary in the range between 13 and 70 % depending on the method. They defined FSP in two different terms: hygroscopic limit (HL) and cell-wall saturation (CWS) including capillary condensed water. In their own investigations, CWS of approximately 34 % for pine or beech and 46 % for spruce could be determined. Hill et al. (2005) determined FSP of 40 % for Corsican pine using the technique of solute exclusion.

Hence, by specification of FSP it should be noted, for better understanding, that it is important from which state (hygroscopic range or water saturated) the values were determined.

Conclusion

The DSC measurements of this work, assuming a melting point depression of water in very small pores, have established that thermal modification of wood leads to decreased nano-pore shares, below a pore diameter of 400 nm, and decreased FSP. In addition to the chemical alteration and degradation of the cell-wall components as well as the formation of fungicidal substances during the thermal modification process, both these phenomena are probably responsible for improving the biological durability. From the results it can be derived that the ratio of capillary condensed water in thermally modified wood is reduced significantly. Thus, the activity of wood decaying fungi is reduced and can be one important reason for the improved durability of thermally modified wood compared to native wood. The results clearly show that milled wood (particles), both native and thermally modified wood, always has higher pore shares in the nano-diameter range and higher FSP compared to solid wood (cross-cut sections). That means, the results significantly depend on the sample shape. A comparison of the native wood samples with each other shows that maple has somewhat lower pore shares in the investigated pore range between approximately 4 and 400 nm compared to spruce and ash. Furthermore, for the calculation of the individual pore size corresponding pore volume, it is important to consider sensible heat due to the inertia of the sample. Otherwise, the calculated pore proportions are falsely too high. For calculating FSP, a separate linear regression method between heat of fusion and moisture content of the samples appears most suitable because in this connection realistic specific heats of fusion are obtained. The measured FSP are higher than the generally assumed FSP of 30 %. This could be explained by the water saturated state of the samples during measurement.

Acknowledgments This publication is based on tests and results that were financially supported by the German Research Foundation (DFG WA 1540/7-2).

References

- Almeida G, Hernández RE (2006) Changes in physical properties of tropical and temperate hardwoods below and above the fiber saturation point. *Wood Sci Technol* 40:599–613
- Aristov YI, Kovalevskaya YA, Tokarev MM, Paukov IE (2010) Low temperature heat capacity of the system “silica gel–calcium chloride–water”. *J Therm Anal Calorim* 103:773–778
- Babiak M, Kudela J (1995) A contribution to the definition of the fiber saturation point. *Wood Sci Technol* 29:217–226
- Chen CM, Wangaard F (1968) Wettability and the hysteresis effect in the sorption of water vapor by wood. *Wood Sci Technol* 2:177–187
- Dieste A, Krause A, Mai C, Sèbe G, Grelier S, Militz H (2009) Modification of *Fagus sylvatica* L. with 1,3-dimethylol-4,5-dihydroxy ethylene urea (DMDHEU). Part 2: pore size distribution determined by differential scanning calorimetry. *Holzforschung* 63:89–93

- Fahlén J, Salmén L (2005) Ultrastructural changes in a holocellulose pulp revealed by enzymes, thermoporosimetry and atomic force microscopy. *Holzforschung* 59:589–597
- Hill CAS (2006) Wood modification. Chemical thermal and other processes. Wiley, Chichester
- Hill CAS (2008) The reduction in the fibre saturation point of wood due to chemical modification using anhydride reagents: a reappraisal. *Holzforschung* 62:423–428
- Hill CAS, Forster SC, Farahani MRM, Hale MDC, Ormondroyd GA, Williams GR (2005) An investigation of cell wall micropore blocking as a possible mechanism for the decay resistance of anhydride modified wood. *Int Biodeterior Biodegrad* 55:69–76
- Kollmann F, Fengel D (1965) Änderungen der chemischen Zusammensetzung von Holz durch thermische Behandlung. *Holz Roh Werkst* 23:461–468
- Książczak A, Radomski A, Zielenkiewicz T (2003) Nitrocellulose porosity—thermoporometry. *J Therm Anal Calorim* 74:559–568
- Kürschner K, Melcerová A (1965) Über die chemischen Veränderungen des Buchenholzes bei thermischer Behandlung. Teil I. Chemische Veränderungen von Sägespänen bei 1–28 tägiger Erhitzung auf 80–160 °C. *Holzforschung* 19:161–171
- Landry M (2005) Thermoporometry by differential scanning calorimetry: experimental considerations and applications. *Thermochim Acta* 433:27–50
- Lekounougou S (2009) Effect of heat treatment on extracellular enzymatic activities involved in beech wood degradation by *Trametes versicolor*. *Wood Sci Technol* 43:331–341
- Maloney T (2000) Messen der Porengrößenverteilung mittels DSC. *UserCom Mettler Toledo* 12:15–17
- Maloney TC, Paulapuro H (1999) The formation of pores in the cell wall. *J Pulp Pap Sci* 25:430–436
- Park S, Venditti R, Jameel H, Pawlak J (2006) Changes in pore size distribution during the drying of cellulose fibers as measured by differential scanning calorimetry. *Carbohydr Polym* 66:97–103
- Peters J, Fischer K, Fischer S (2008) Characterization of emissions from thermally modified wood and their reduction by chemical treatment. *Bioresources* 3:491–502
- Pétrissans A, Younsi R, Chaouch M, Gérardin P, Pétrissans M (2012) Experimental and numerical analysis of wood thermodegradation: mass loss kinetics. *J Therm Anal Calorim* 109:907–914
- Repellin V, Guyonnet R (2005) Evaluation of heat-treated wood swelling by differential scanning calorimetry in relation to chemical composition. *Holzforschung* 59:28–34
- Roffael E, Kraft R (2012) Einfluss der thermischen Modifizierung von Holz auf das Wasser-rückhaltevermögen (WRV-Wert). *Eur J Wood Prod* 70:393–395
- Siau J (1995) Wood: influence of moisture on physical properties. Virginia Polytechnic Institute and State University, VA
- Simpson L, Barton AFM (1991) Determination of the fibre saturation point in whole wood using differential scanning calorimetry. *Wood Sci Technol* 25:301–308
- Stephan P, Schaber K, Stephan K, Mayinger F (2010) *Thermodynamik. Grundlagen und Technische Anwendungen*. Springer, Heidelberg
- Tjeerdsma BF, Boonstra M, Pizzi A, Tekely P, Militz H (1998) Characterisation of thermally modified wood: molecular reasons for wood performance improvement. *Holz Roh Werkst* 56:149–153
- Topgaard D, Söderman O (2002) Self-diffusion of nonfreezing water in porous carbohydrate polymer systems studied with nuclear magnetic resonance. *Biophys J* 83:3596–3606
- Wagenführ A, Scholz F (2007) *Taschenbuch der Holztechnik*. Hanser Fachbuch, München
- Weise U, Maloney T, Paulapuro H (1996) Quantification of water in different states of interaction with wood pulp fibres. *Cellulose* 3:189–202
- Zauer M (2011) Untersuchung zur Porenstruktur und kapillaren Wasserleitung im Holz und deren Änderung infolge einer thermischen Modifikation. Doctoral thesis, TU Dresden
- Zauer M, Pfriem A, Wagenführ A (2013) Toward improved understanding of the cell-wall density and porosity of wood determined by gas pycnometry. *Wood Sci Technol* 47(6):1197–1211
- Zelinka SL, Lambrecht MJ, Glass SV, Wiedenhoeft AC, Yelle DJ (2012) Examination of water phase transition in Loblolly pine and cell wall components by differential scanning calorimetry. *Thermochim Acta* 533:38–45